

Observation of the Electroweak Penguin Decay $B \rightarrow K^* \ell^+ \ell^-$

K. Abe,⁹ K. Abe,⁴⁴ N. Abe,⁴⁷ R. Abe,³⁰ T. Abe,⁹ I. Adachi,⁹ Byoung Sup Ahn,¹⁶
H. Aihara,⁴⁶ M. Akatsu,²³ M. Asai,¹⁰ Y. Asano,⁵¹ T. Aso,⁵⁰ V. Aulchenko,² T. Aushev,¹³
S. Bahinipati,⁵ A. M. Bakich,⁴¹ Y. Ban,³⁴ E. Banas,²⁸ S. Banerjee,⁴² A. Bay,¹⁹
I. Bedny,² P. K. Behera,⁵² I. Bizjak,¹⁴ A. Bondar,² A. Bozek,²⁸ M. Bračko,^{21,14}
J. Brodzicka,²⁸ T. E. Browder,⁸ M.-C. Chang,²⁷ P. Chang,²⁷ Y. Chao,²⁷ K.-F. Chen,²⁷
B. G. Cheon,⁴⁰ R. Chistov,¹³ S.-K. Choi,⁷ Y. Choi,⁴⁰ Y. K. Choi,⁴⁰ M. Danilov,¹³
M. Dash,⁵³ E. A. Dodson,⁸ L. Y. Dong,¹¹ R. Dowd,²² J. Dragic,²² A. Drutskoy,¹³
S. Eidelman,² V. Eiges,¹³ Y. Enari,²³ D. Epifanov,² C. W. Everton,²² F. Fang,⁸ H. Fujii,⁹
C. Fukunaga,⁴⁸ N. Gabyshev,⁹ A. Garmash,^{2,9} T. Gershon,⁹ G. Gokhroo,⁴² B. Golob,^{20,14}
A. Gordon,²² M. Grosse Perdekamp,³⁶ H. Guler,⁸ R. Guo,²⁵ J. Haba,⁹ C. Hagner,⁵³
F. Handa,⁴⁵ K. Hara,³² T. Hara,³² Y. Harada,³⁰ N. C. Hastings,⁹ K. Hasuko,³⁶
H. Hayashii,²⁴ M. Hazumi,⁹ E. M. Heenan,²² I. Higuchi,⁴⁵ T. Higuchi,⁹ L. Hinz,¹⁹
T. Hojo,³² T. Hokuue,²³ Y. Hoshi,⁴⁴ K. Hoshina,⁴⁹ W.-S. Hou,²⁷ Y. B. Hsiung,^{27,*}
H.-C. Huang,²⁷ T. Igaki,²³ Y. Igarashi,⁹ T. Iijima,²³ K. Inami,²³ A. Ishikawa,²³ H. Ishino,⁴⁷
R. Itoh,⁹ M. Iwamoto,³ H. Iwasaki,⁹ M. Iwasaki,⁴⁶ Y. Iwasaki,⁹ H. K. Jang,³⁹ R. Kagan,¹³
H. Kakuno,⁴⁷ J. Kaneko,⁴⁷ J. H. Kang,⁵⁵ J. S. Kang,¹⁶ P. Kapusta,²⁸ M. Kataoka,²⁴
S. U. Kataoka,²⁴ N. Katayama,⁹ H. Kawai,³ H. Kawai,⁴⁶ Y. Kawakami,²³ N. Kawamura,¹
T. Kawasaki,³⁰ N. Kent,⁸ A. Kibayashi,⁴⁷ H. Kichimi,⁹ D. W. Kim,⁴⁰ Heejong Kim,⁵⁵
H. J. Kim,⁵⁵ H. O. Kim,⁴⁰ Hyunwoo Kim,¹⁶ J. H. Kim,⁴⁰ S. K. Kim,³⁹ T. H. Kim,⁵⁵
K. Kinoshita,⁵ S. Kobayashi,³⁷ P. Koppenburg,⁹ K. Korotushenko,³⁵ S. Korpar,^{21,14}
P. Križan,^{20,14} P. Krokovny,² R. Kulasiri,⁵ S. Kumar,³³ E. Kurihara,³ A. Kusaka,⁴⁶
A. Kuzmin,² Y.-J. Kwon,⁵⁵ J. S. Lange,^{6,36} G. Leder,¹² S. H. Lee,³⁹ T. Lesiak,²⁸
J. Li,³⁸ A. Limosani,²² S.-W. Lin,²⁷ D. Liventsev,¹³ R.-S. Lu,²⁷ J. MacNaughton,¹²
G. Majumder,⁴² F. Mandl,¹² D. Marlow,³⁵ T. Matsubara,⁴⁶ T. Matsuishi,²³
H. Matsumoto,³⁰ S. Matsumoto,⁴ T. Matsumoto,⁴⁸ A. Matyja,²⁸ Y. Mikami,⁴⁵
W. Mitaroff,¹² K. Miyabayashi,²⁴ Y. Miyabayashi,²³ H. Miyake,³² H. Miyata,³⁰
L. C. Moffitt,²² D. Mohapatra,⁵³ G. R. Moloney,²² G. F. Moorhead,²² S. Mori,⁵¹ T. Mori,⁴⁷
J. Mueller,^{9,†} A. Murakami,³⁷ T. Nagamine,⁴⁵ Y. Nagasaka,¹⁰ T. Nakadaira,⁴⁶ E. Nakano,³¹
M. Nakao,⁹ H. Nakazawa,⁹ J. W. Nam,⁴⁰ S. Narita,⁴⁵ Z. Natkaniec,²⁸ K. Neichi,⁴⁴
S. Nishida,⁹ O. Nitoh,⁴⁹ S. Noguchi,²⁴ T. Nozaki,⁹ A. Ogawa,³⁶ S. Ogawa,⁴³ F. Ohno,⁴⁷
T. Ohshima,²³ T. Okabe,²³ S. Okuno,¹⁵ S. L. Olsen,⁸ Y. Onuki,³⁰ W. Ostrowicz,²⁸
H. Ozaki,⁹ P. Pakhlov,¹³ H. Palka,²⁸ C. W. Park,¹⁶ H. Park,¹⁸ K. S. Park,⁴⁰ N. Parslow,⁴¹
L. S. Peak,⁴¹ M. Pernicka,¹² J.-P. Perroud,¹⁹ M. Peters,⁸ L. E. Pilonen,⁵³ F. J. Ronga,¹⁹
N. Root,² M. Rozanska,²⁸ H. Sagawa,⁹ S. Saitoh,⁹ Y. Sakai,⁹ H. Sakamoto,¹⁷ H. Sakaue,³¹
T. R. Sarangi,⁵² M. Satapathy,⁵² A. Satpathy,^{9,5} O. Schneider,¹⁹ S. Schrenk,⁵
J. Schümann,²⁷ C. Schwanda,^{9,12} A. J. Schwartz,⁵ T. Seki,⁴⁸ S. Semenov,¹³ K. Senyo,²³
Y. Settai,⁴ R. Seuster,⁸ M. E. Sevir,²² T. Shibata,³⁰ H. Shibuya,⁴³ M. Shimoyama,²⁴
B. Shwartz,² V. Sidorov,² V. Siegle,³⁶ J. B. Singh,³³ N. Soni,³³ S. Stanič,^{51,‡} M. Starič,¹⁴
A. Sugi,²³ A. Sugiyama,³⁷ K. Sumisawa,⁹ T. Sumiyoshi,⁴⁸ K. Suzuki,⁹ S. Suzuki,⁵⁴

S. Y. Suzuki,⁹ S. K. Swain,⁸ K. Takahashi,⁴⁷ F. Takasaki,⁹ B. Takeshita,³² K. Tamai,⁹
 Y. Tamai,³² N. Tamura,³⁰ K. Tanabe,⁴⁶ J. Tanaka,⁴⁶ M. Tanaka,⁹ G. N. Taylor,²²
 A. Tchouvikov,³⁵ Y. Teramoto,³¹ S. Tokuda,²³ M. Tomoto,⁹ T. Tomura,⁴⁶ S. N. Tovey,²²
 K. Trabelsi,⁸ T. Tsuboyama,⁹ T. Tsukamoto,⁹ K. Uchida,⁸ S. Uehara,⁹ K. Ueno,²⁷
 T. Uglov,¹³ Y. Unno,³ S. Uno,⁹ N. Uozaki,⁴⁶ Y. Ushiroda,⁹ S. E. Vahsen,³⁵ G. Varner,⁸
 K. E. Varvell,⁴¹ C. C. Wang,²⁷ C. H. Wang,²⁶ J. G. Wang,⁵³ M.-Z. Wang,²⁷
 M. Watanabe,³⁰ Y. Watanabe,⁴⁷ L. Widhalm,¹² E. Won,¹⁶ B. D. Yabsley,⁵³ Y. Yamada,⁹
 A. Yamaguchi,⁴⁵ H. Yamamoto,⁴⁵ T. Yamanaka,³² Y. Yamashita,²⁹ Y. Yamashita,⁴⁶
 M. Yamauchi,⁹ H. Yanai,³⁰ Heyoung Yang,³⁹ J. Yashima,⁹ P. Yeh,²⁷ M. Yokoyama,⁴⁶
 K. Yoshida,²³ Y. Yuan,¹¹ Y. Yusa,⁴⁵ H. Yuta,¹ C. C. Zhang,¹¹ J. Zhang,⁵¹ Z. P. Zhang,³⁸
 Y. Zheng,⁸ V. Zhilich,² Z. M. Zhu,³⁴ T. Ziegler,³⁵ D. Žontar,^{20,14} and D. Zürcher¹⁹

(The Belle Collaboration)

¹*Aomori University, Aomori*

²*Budker Institute of Nuclear Physics, Novosibirsk*

³*Chiba University, Chiba*

⁴*Chuo University, Tokyo*

⁵*University of Cincinnati, Cincinnati, Ohio 45221*

⁶*University of Frankfurt, Frankfurt*

⁷*Gyeongsang National University, Chinju*

⁸*University of Hawaii, Honolulu, Hawaii 96822*

⁹*High Energy Accelerator Research Organization (KEK), Tsukuba*

¹⁰*Hiroshima Institute of Technology, Hiroshima*

¹¹*Institute of High Energy Physics,*

Chinese Academy of Sciences, Beijing

¹²*Institute of High Energy Physics, Vienna*

¹³*Institute for Theoretical and Experimental Physics, Moscow*

¹⁴*J. Stefan Institute, Ljubljana*

¹⁵*Kanagawa University, Yokohama*

¹⁶*Korea University, Seoul*

¹⁷*Kyoto University, Kyoto*

¹⁸*Kyungpook National University, Taegu*

¹⁹*Institut de Physique des Hautes Énergies, Université de Lausanne, Lausanne*

²⁰*University of Ljubljana, Ljubljana*

²¹*University of Maribor, Maribor*

²²*University of Melbourne, Victoria*

²³*Nagoya University, Nagoya*

²⁴*Nara Women's University, Nara*

²⁵*National Kaohsiung Normal University, Kaohsiung*

²⁶*National Lien-Ho Institute of Technology, Miao Li*

²⁷*Department of Physics, National Taiwan University, Taipei*

²⁸*H. Niewodniczanski Institute of Nuclear Physics, Krakow*

²⁹*Nihon Dental College, Niigata*

³⁰*Niigata University, Niigata*

³¹*Osaka City University, Osaka*

³²*Osaka University, Osaka*

- ³³*Panjab University, Chandigarh*
³⁴*Peking University, Beijing*
³⁵*Princeton University, Princeton, New Jersey 08545*
³⁶*RIKEN BNL Research Center, Upton, New York 11973*
³⁷*Saga University, Saga*
³⁸*University of Science and Technology of China, Hefei*
³⁹*Seoul National University, Seoul*
⁴⁰*Sungkyunkwan University, Suwon*
⁴¹*University of Sydney, Sydney NSW*
⁴²*Tata Institute of Fundamental Research, Bombay*
⁴³*Toho University, Funabashi*
⁴⁴*Tohoku Gakuin University, Tagajo*
⁴⁵*Tohoku University, Sendai*
⁴⁶*Department of Physics, University of Tokyo, Tokyo*
⁴⁷*Tokyo Institute of Technology, Tokyo*
⁴⁸*Tokyo Metropolitan University, Tokyo*
⁴⁹*Tokyo University of Agriculture and Technology, Tokyo*
⁵⁰*Toyama National College of Maritime Technology, Toyama*
⁵¹*University of Tsukuba, Tsukuba*
⁵²*Utkal University, Bhubaneswer*
⁵³*Virginia Polytechnic Institute and State University, Blacksburg, Virginia 24061*
⁵⁴*Yokkaichi University, Yokkaichi*
⁵⁵*Yonsei University, Seoul*

Abstract

We report the first observation of the electroweak penguin decay $B \rightarrow K^* \ell^+ \ell^-$ and an improved measurement of the decay $B \rightarrow K \ell^+ \ell^-$, where ℓ represents an electron or a muon, with a data sample of 140 fb^{-1} accumulated on the $\Upsilon(4S)$ resonance with the Belle detector at KEKB. The preliminary results for the branching fractions are $\mathcal{B}(B \rightarrow K \ell^+ \ell^-) = (4.8_{-0.9}^{+1.0} \pm 0.3 \pm 0.1) \times 10^{-7}$ and $\mathcal{B}(B \rightarrow K^* \ell^+ \ell^-) = (11.5_{-2.4}^{+2.6} \pm 0.7 \pm 0.4) \times 10^{-7}$, where the first error is statistical, the second is systematic and the third is model dependence.

PACS numbers: 13.20.He, 11.30.Hv

Flavor-changing neutral current (FCNC) processes are forbidden at tree level in the Standard Model (SM); rather, they proceed at a low rate via loop or box diagrams. If additional such diagrams with non-SM particles contribute to such a decay, their amplitudes will interfere with the SM amplitudes and thereby modify FCNC decay rate. This feature makes FCNC processes an ideal place to search for new physics.

Measurements of the radiative penguin decay $B \rightarrow X_s \gamma$ [1, 2, 3], which are consistent with the SM prediction, strongly constrain the magnitude—but not the sign—of the effective Wilson coefficient C_7 . This is an important limitation, since non-SM contributions can change the sign of C_7 without changing the $B \rightarrow X_s \gamma$ branching fraction [4].

The $b \rightarrow s \ell^+ \ell^-$ process is promising from this point of view, since not only the photonic penguin diagram but also the Z -penguin and box diagrams contribute to this decay mode. As a result, the Wilson coefficients C_7 , C_9 and C_{10} can be completely determined. The first observation of $B \rightarrow K \ell^+ \ell^-$ and the first measurement of inclusive $B \rightarrow X_s \ell^+ \ell^-$ decays were reported by the Belle Collaboration [5, 6] and were used to exclude a large area of allowed region in C_9 - C_{10} plane [7, 8]. However, a precise determination of all three Wilson coefficients depends on the measurement of the forward-backward asymmetry in $B \rightarrow K^* \ell^+ \ell^-$ [9].

In this paper, we present preliminary results of a search for $B \rightarrow K^* \ell^+ \ell^-$ and an improved measurement of $B \rightarrow K \ell^+ \ell^-$ using data produced in e^+e^- annihilation at the KEKB asymmetric collider [10] and collected with the Belle detector. The data sample corresponds to 140 fb^{-1} taken at the $\Upsilon(4S)$ resonance and contains approximately 152 million $B\bar{B}$ pairs.

Belle is a general-purpose detector based on a 1.5 T superconducting solenoid magnet that surrounds the KEKB beam crossing point. Charged particle tracking covering approximately 90% of the total center-of-mass (CM) solid angle is provided by a Silicon Vertex Detector (SVD), consisting of three nearly cylindrical layers of double-sided silicon strip detectors, and a 50-layer Central Drift Chamber (CDC). Particle identification is accomplished by a combination of a silica Aerogel Cherenkov Counters (ACC), a Time of Flight counter system (TOF) and specific ionization measurements (dE/dx) in the CDC. A CsI(Tl) Electromagnetic Calorimeter (ECL) located inside the solenoid coil is used for γ/π^0 detection and electron identification. The μ/K_L detector (KLM) is located outside of the coil. An Extreme Forward Calorimeter (EFC) is situated near the beam pipe. A detailed description of the Belle detector can be found elsewhere [11].

In this analysis, primary charged tracks—except for the daughters from $K_S \rightarrow \pi^+ \pi^-$ decays—are required to have impact parameters relative to the interaction point of less than 5.0 cm along the z axis (aligned along the positron beam) and less than 0.5 cm in the $r\phi$ plane that is transverse to this axis. This requirement reduces the combinatorial background from photon conversion, beam-gas and beam-wall events.

Charged tracks are identified as either kaons and pions by a likelihood ratio based on the CDC specific ionization, time-of-flight information and the light yield in the ACC. This classification is superceded for a track that is identified as an electron or for a pion-like track that is identified as a muon. Electrons are identified from the ratio of shower energy of the matching ECL cluster to the momentum measured by the CDC, the transverse shower shape of this cluster, the specific ionization in the CDC and the ACC response. We require that the electron momentum be greater than 0.4 GeV/ c to reach the ECL. Muons are identified by their penetration depth and transverse scattering in the KLM. The muon momentum is required to exceed 0.7 GeV/ c . The muon identification criteria are more stringent for momenta below 1.0 GeV/ c to suppress misidentified hadrons.

Photons are selected from isolated neutral clusters in the ECL with energy greater than

50 MeV and a shape that is consistent with an electromagnetic shower. Neutral pion candidates are reconstructed from pairs of photons, and are required to have an invariant mass within $10 \text{ MeV}/c^2$ of the nominal π^0 mass and a laboratory momentum greater than $0.1 \text{ GeV}/c$. K_S^0 candidates are reconstructed from oppositely charged pions with a vertex displaced from the interaction point and an invariant mass within $15 \text{ MeV}/c^2$ of the nominal K_S^0 mass.

K^* candidates are formed by combining a kaon and a pion: $K^+\pi^-$, $K_S^0\pi^+$ or $K^+\pi^0$ [12]. The K^* invariant mass is required to lie within $75 \text{ MeV}/c^2$ of the nominal K^* mass. For modes involving neutral pions, combinatorial backgrounds are reduced by the additional requirement $\cos\theta_{\text{hel}} < 0.8$, where θ_{hel} is defined as the angle between the K^* momentum direction and the kaon momentum direction in the K^* rest frame.

B candidates are reconstructed from a $K^{(*)}$ candidate and an oppositely-charged lepton pair. We use two variables defined in the CM frame to select B candidates: the beam-energy constrained mass $M_{\text{bc}} = \sqrt{E_{\text{beam}}^2 - p_B^2}$ and the energy difference $\Delta E = E_B - E_{\text{beam}}$, where p_B and E_B are the measured momentum and energy, respectively, of the B candidate, and E_{beam} is the beam energy. When multiple candidates are found in a event, we select the candidate with the smallest value of $|\Delta E|$.

Backgrounds from $B \rightarrow J/\psi(\psi')K^{(*)}$ are rejected using the dilepton invariant mass. The veto windows are defined as

$$\begin{aligned}
-0.25 < M_{e^+e^-} - M_{J/\psi} < 0.07 \text{ GeV}/c^2 & \quad \text{for } K^* \text{ modes} \\
-0.20 < M_{e^+e^-} - M_{J/\psi} < 0.07 \text{ GeV}/c^2 & \quad \text{for } K \text{ modes} \\
-0.20 < M_{e^+e^-} - M_{\psi'} < 0.07 \text{ GeV}/c^2 & \quad \text{for } K^* \text{ and } K \text{ modes} \\
-0.15 < M_{\mu^+\mu^-} - M_{J/\psi} < 0.08 \text{ GeV}/c^2 & \quad \text{for } K^* \text{ modes} \\
-0.10 < M_{\mu^+\mu^-} - M_{J/\psi} < 0.08 \text{ GeV}/c^2 & \quad \text{for } K \text{ modes} \\
-0.10 < M_{\mu^+\mu^-} - M_{\psi'} < 0.08 \text{ GeV}/c^2 & \quad \text{for } K^* \text{ and } K \text{ modes}
\end{aligned}$$

If a photon with energy less than 500 MeV is found in the 50 mrad cone along the electron momentum direction, we also use the invariant mass calculated including this photon to reject the background with a bremsstrahlung photon, $J/\psi(\psi') \rightarrow e^+e^-\gamma(\gamma)$. For $K^*e^+e^-$ modes, $B \rightarrow J/\psi K$ can be a background if a bremsstrahlung photon is missed and a pion from the the other B in the event is included. We suppress this background by the following prescription: the included pion is discarded and an unobserved bremsstrahlung photon is added with a direction parallel to one or the other electron and an energy that gives $\Delta E = 0$ for the B candidate. If the dilepton mass and the beam-energy constrained mass are consistent with a $B \rightarrow J/\psi K$ event, the candidate is vetoed.

We suppress background from photon conversions and π^0 Dalitz decays by requiring the dielectron mass to satisfy $M_{e^+e^-} > 0.14 \text{ GeV}/c^2$. This cut eliminates possible peaking background from $B \rightarrow K^*\gamma$ and $B \rightarrow K^{(*)}\pi^0$.

Background from continuum $q\bar{q}$ events is suppressed using event topology. Continuum events have a jet-like shape while $B\bar{B}$ events have a spherical shape in the center-of-mass frame. A Fisher discriminant \mathcal{F} [13] is calculated from the energy flow in 9 cones along the B candidate sphericity axis and the normalized second Fox-Wolfram moment R_2 [14]. We combine this with the cosine of the polar angle $\cos\theta_B$ of the B meson flight direction and the cosine of the angle between B meson sphericity axis and the z axis, $\cos\theta_{\text{sph}}$, to define likelihoods \mathcal{L}_{sig} and $\mathcal{L}_{\text{cont}}$ for signal and continuum background, respectively, and then cut on the likelihood ratio $\mathcal{LR}_{\text{cont}} = \mathcal{L}_{\text{sig}}/(\mathcal{L}_{\text{sig}} + \mathcal{L}_{\text{cont}})$. For the muon mode, $|\cos\theta_{\text{sph}}|$ is not used since its distribution is nearly the same for signal and continuum within the detector acceptance.

The dominant background from $B\bar{B}$ events is due to semileptonic B decays. The missing energy of the event, E_{miss} , is used to suppress the background since we expect a large amount of missing energy due to the undetected neutrinos. The B meson flight angle is also used to suppress combinatorial background in $B\bar{B}$ events. We combine E_{miss} and $\cos\theta_B$ into signal and $B\bar{B}$ -background likelihoods and cut on the likelihood ratio $\mathcal{LR}_{B\bar{B}}$, defined similarly to $\mathcal{LR}_{\text{cont}}$.

The selection criteria are tuned to maximize the expected significance $S/\sqrt{S+B}$, where S is the signal yield and B is the expected background in the signal box. S and B are determined from GEANT based Monte Carlo (MC) samples. The $B \rightarrow K^{(*)}\ell^+\ell^-$ decays are generated with several models [7, 15, 16] to estimate the efficiencies. The signal box is defined as $|M_{\text{bc}} - M_B| < 0.007 \text{ GeV}/c^2$ for both lepton modes and $-0.055 < \Delta E < 0.035 \text{ GeV}$ ($|\Delta E| < 0.035 \text{ GeV}$) for the electron (muon) mode. We make distinct selections on $\mathcal{LR}_{\text{cont}}$ and $\mathcal{LR}_{B\bar{B}}$ for each decay mode. The detection efficiencies are estimated using MC samples and summarized in Table II. Figure 1 shows the event distributions over the ΔE vs. M_{bc} plane for each mode.

To determine the signal yield, we perform a binned maximum-likelihood fit to each M_{bc} distribution. The expected number of signal events is calculated as a function of M_{bc} using a Gaussian signal distribution plus background functions. The mean and the width of the signal Gaussian are determined using observed $J/\psi K^{(*)}$ events. A MC study shows that the width has no dependence on the dilepton invariant mass. We consider three backgrounds: background from semileptonic decays, J/ψ and ψ' , and double misidentification of hadrons as leptons. The background from semileptonic decays is parameterized by the ARGUS function [17]. The shape is determined from several large MC samples, each containing at least one oppositely charged lepton pair. The shape parameter obtained from MC is consistent with the shape taken from a data sample of $B \rightarrow K^{(*)}e^\pm\mu^\mp$ candidates. The residual background from J/ψ and ψ' mesons that evade the $\psi^{(\prime)}$ veto windows is estimated from a large MC sample of J/ψ and ψ' inclusive events and parameterized by an ARGUS function plus a Gaussian. The background contribution due to misidentification of hadrons as leptons is parameterized by another ARGUS function plus a Gaussian. The ARGUS function represents the combinatorial background while the Gaussian represents the component that makes a peak in the M_{bc} distribution. The shape and normalization of this background are fixed using the $B \rightarrow K^{(*)}h^+h^-$ data sample (h refers to a pion or kaon). All $K^{(*)}h^+h^-$ combinations are weighted by the momentum and polar angle dependent probability of misidentifying $K^{(*)}h^+h^-$ as $K^{(*)}\ell^+\ell^-$. This study yields $1.05 \pm 0.08 K h^+ h^-$ events and $0.64 \pm 0.05 K^* h^+ h^-$ events in the peak region. Other backgrounds with misidentified leptons are negligible. The normalizations of the signal and the background from real leptons are allowed to float in the fit. The fit results are shown in Figure 2 and 3 and summarized in Table II.

We observe $35.8_{-6.9}^{+7.6} B \rightarrow K^*\ell^+\ell^-$ signal with a significance of 5.9 and $37.9_{-6.9}^{+7.6} B \rightarrow K\ell^+\ell^-$ signal with a significance of 7.4. The significance is defined as $\sqrt{-2\ln(\mathcal{L}_0/\mathcal{L}_{\text{max}})}$, where \mathcal{L}_{max} is the maximum likelihood in the M_{bc} fit and \mathcal{L}_0 is the likelihood of the best fit when the signal yield is constrained to be zero. Since the signal and background shapes are fixed in the fitting, the error due to uncertainty in shape parameters is included in the systematic error. We determine this by varying each shape parameter by $\pm 1\sigma$ and recalculating the signal yield. We quote the smallest resulting significance in our determinations above.

We also measure the q^2 distributions in $B \rightarrow K\ell^+\ell^-$ and $K^*\ell^+\ell^-$. The signal yield is extracted in each q^2 bin from a fit to the M_{bc} distributions. Fig. 4 shows the q^2 distributions

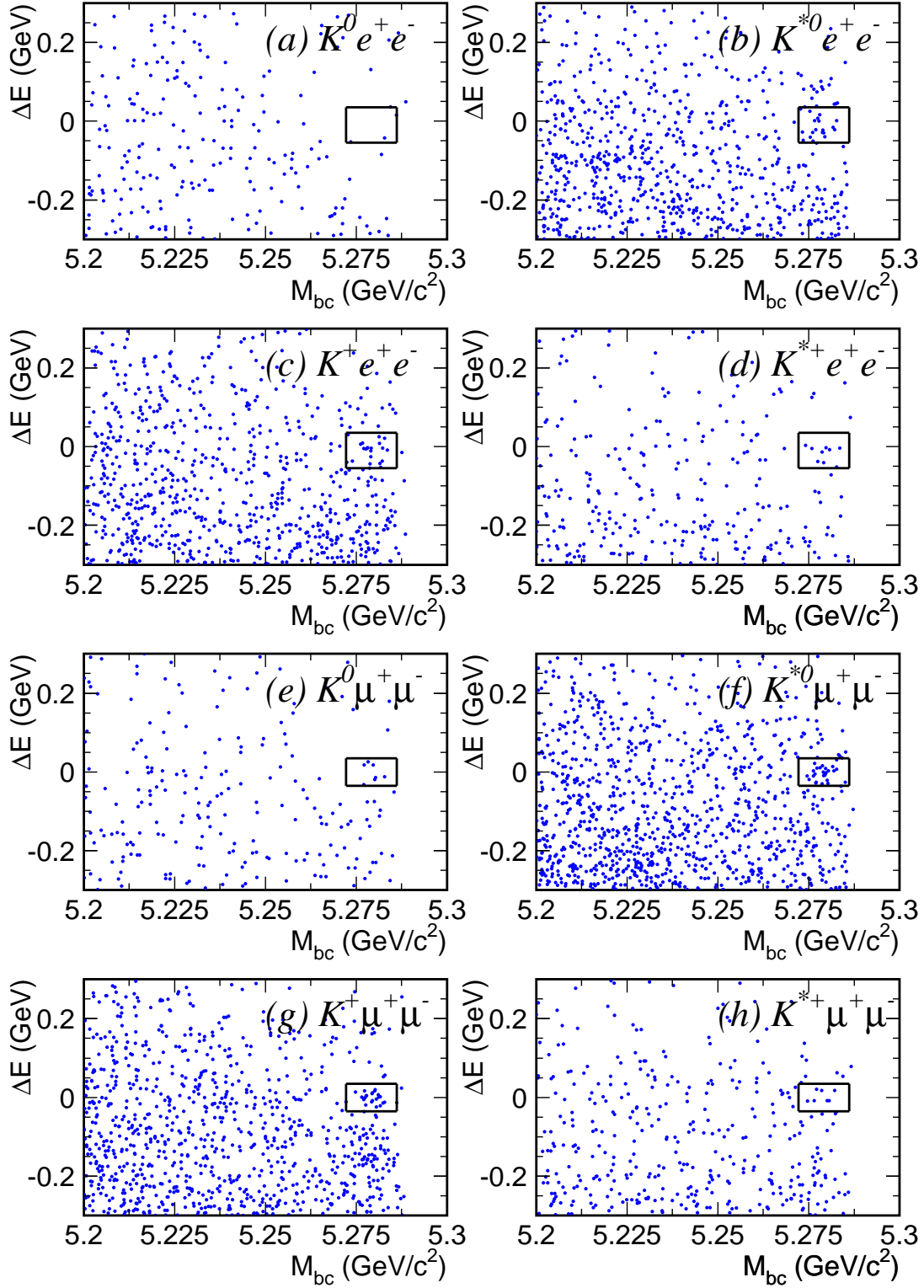


FIG. 1: Event distribution over the ΔE vs. M_{bc} plane for (a) $B^0 \rightarrow K^0 e^+ e^-$, (b) $B^0 \rightarrow K^{*0} e^+ e^-$, (c) $B^+ \rightarrow K^+ e^+ e^-$, (d) $B^+ \rightarrow K^{*+} e^+ e^-$, (e) $B^0 \rightarrow K^0 \mu^+ \mu^-$, (f) $B^0 \rightarrow K^{*0} \mu^+ \mu^-$, (g) $B^+ \rightarrow K^+ \mu^+ \mu^-$ and (h) $B^+ \rightarrow K^{*+} \mu^+ \mu^-$.

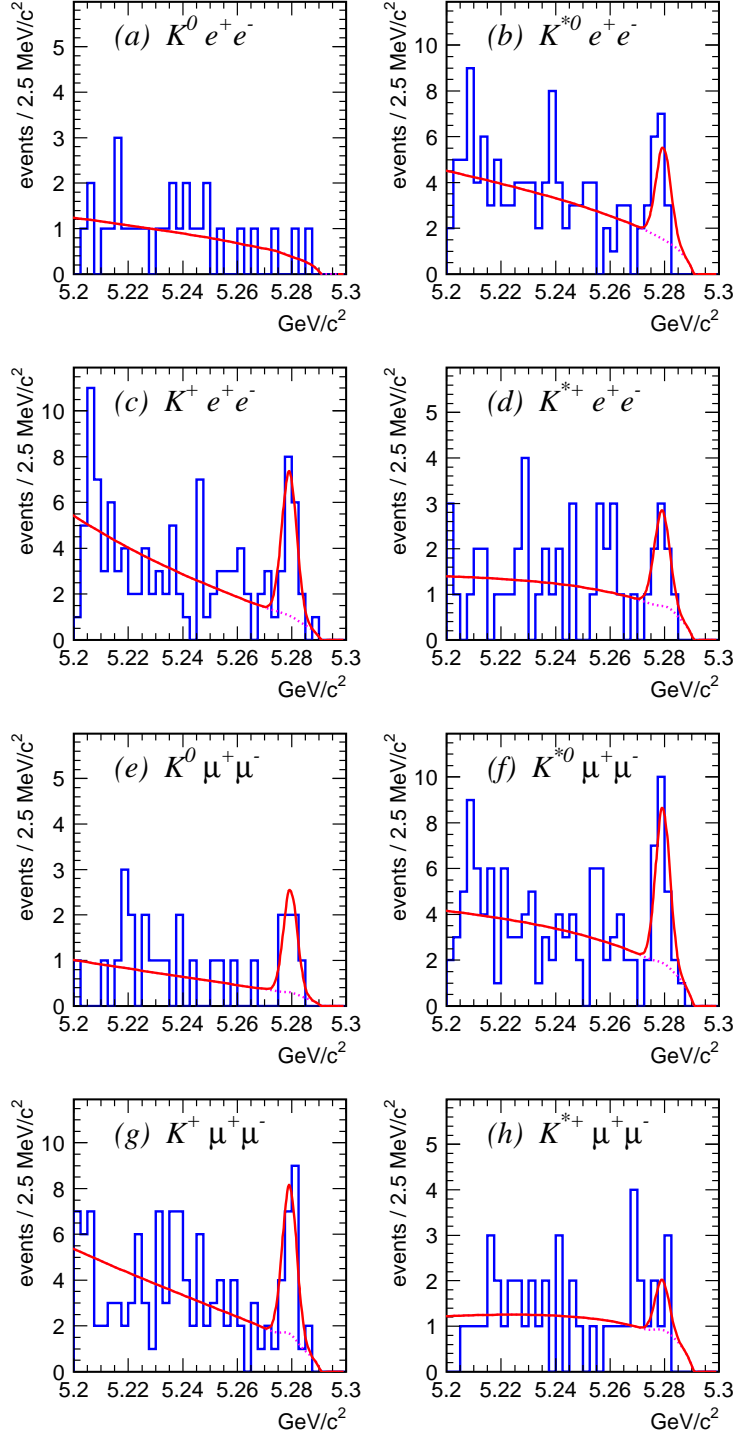


FIG. 2: M_{bc} distributions for (a) $B^0 \rightarrow K^0 e^+ e^-$, (b) $B^0 \rightarrow K^{*0} e^+ e^-$, (c) $B^+ \rightarrow K^+ e^+ e^-$, (d) $B^+ \rightarrow K^{*+} e^+ e^-$, (e) $B^0 \rightarrow K^0 \mu^+ \mu^-$, (f) $B^0 \rightarrow K^{*0} \mu^+ \mu^-$, (g) $B^+ \rightarrow K^+ \mu^+ \mu^-$ and (g) $B^+ \rightarrow K^{*+} \mu^+ \mu^-$. The solid and dotted curves are the fit results of the total and background contributions.

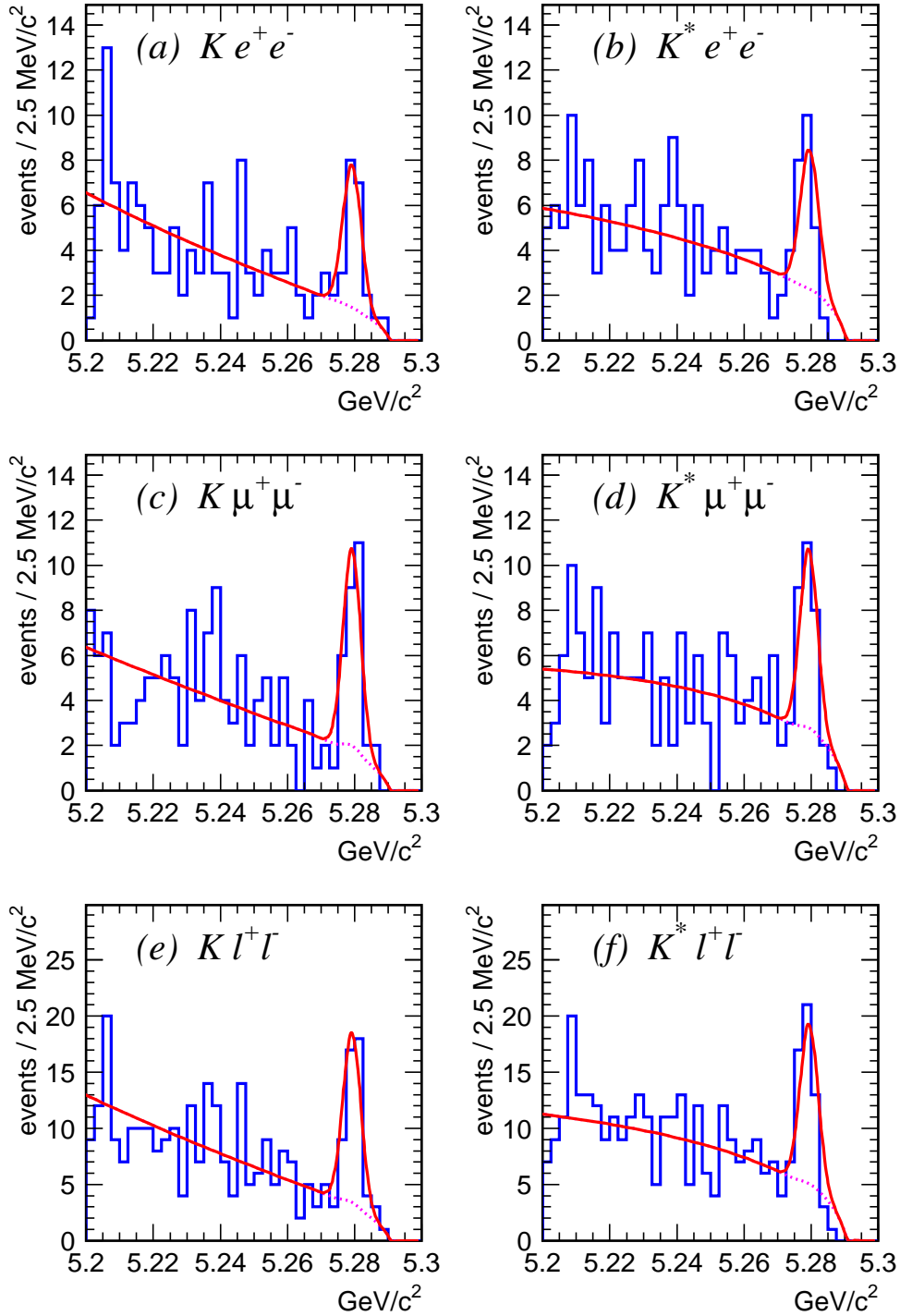


FIG. 3: M_{bc} distributions for (a) $B \rightarrow Ke^+e^-$, (b) $B \rightarrow K^*e^+e^-$, (c) $B \rightarrow K\mu^+\mu^-$, (d) $B \rightarrow K^*\mu^+\mu^-$, (e) $B \rightarrow Kl^+l^-$ and (f) $B \rightarrow K^*l^+l^-$ samples. The solid and dotted curves are the fit results of the total and background contributions.

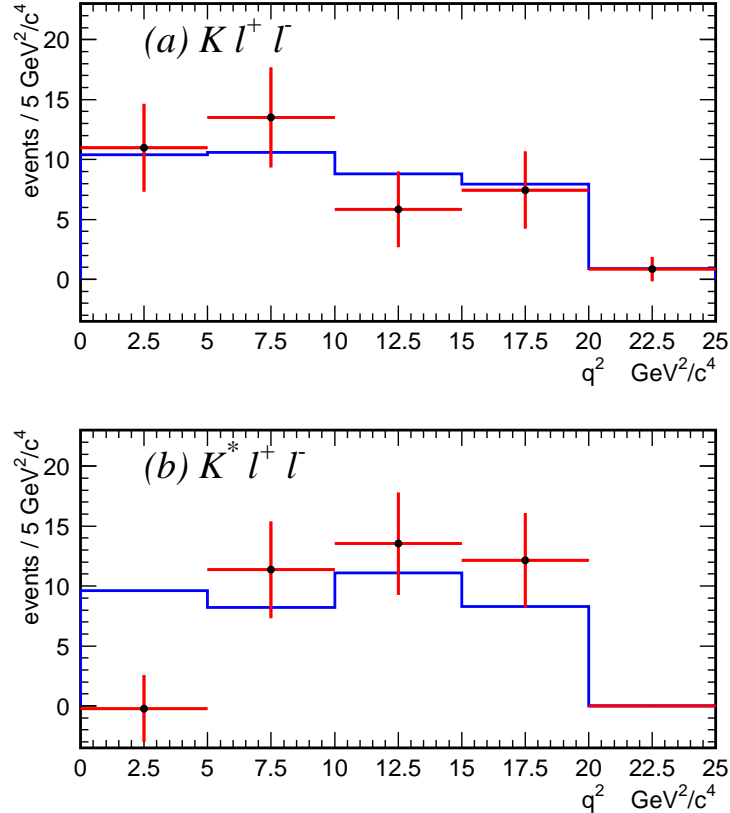


FIG. 4: The q^2 distributions of (a) $K l^+ l^-$ and (b) $K^* l^+ l^-$. Dots with error bars show the data, while the histogram shows MC signal distribution.

for $B \rightarrow K l^- l^-$ and $K^* l^+ l^-$.

We consider experimental systematic effects from the fit, the efficiency determination and $B\bar{B}$ event counting. Uncertainty in the background function is the dominant source of the systematic error. To evaluate the effect of the signal function parameters, the mean and the width of the Gaussian are changed by $\pm 1\sigma$ from the values determined from $J/\psi K^{(*)}$ events. The uncertainty in the background shape is obtained by varying the ARGUS shape parameter by $\pm 1\sigma$ from the value determined with a large MC sample. The uncertainty in peaking background is also evaluated by changing the area of Gaussian by $\pm 1\sigma$. The systematic errors associated with the fit function are shown in the third column of Table II. Systematic uncertainties in the tracking, charged kaon ID, charged pion ID, electron ID, muon ID, K_S^0 detection and π^0 detection efficiencies are estimated to be 1.0%, 1.0%, 0.8%, 0.5%, 1.2%, 4.5% and 2.7% per particle, respectively. The uncertainty in the background suppression is estimated to be 2.3 % using $J/\psi K^{(*)}$ control samples. The uncertainty in $B\bar{B}$ event counting is obtained to be 0.5 %. The systematic errors associated with efficiency and $B\bar{B}$ event counting are summarized in the Table II. Total experimental systematic errors are calculated by adding all systematic errors in quadrature.

The systematics in theoretical model is also evaluated. We apply same selection criteria on the signal samples generated according to three form factor models [7, 15, 16] and obtain the efficiencies. The maximum difference of the efficiency is assigned as uncertainty in model

dependence , which is listed in the fourth column of Table II.

Source	K^0	K^+	$K^+\pi^-$	$K_S^0\pi^+$	$K^+\pi^0$
Tracking	2.0	3.0	4.0	3.0	3.0
Kaon ID	-	1.0	1.0	-	1.0
Pion ID	-	-	0.8	0.8	-
Lepton ID (e/μ)	1.0/2.4	1.0/2.4	1.0/2.4	1.0/2.4	1.0/2.4
K_S^0 detection	4.5	-	-	4.5	-
π^0 detection	-	-	-	-	2.7
BG suppression	2.3	2.3	2.3	2.3	2.3
MC statistics (e/μ)	1.3/1.2	0.7/0.6	1.2/1.1	2.8/2.3	4.0/2.9
$B\bar{B}$ event counting	0.5	0.5	0.5	0.5	0.5
total (e/μ)	5.8/6.1	4.2/4.7	5.1/5.5	6.7/6.8	6.3/6.1

TABLE I: Summary of systematic errors in efficiencies and $B\bar{B}$ event counting.

In calculating the branching fractions, we assume equal fractions of charged and neutral B meson pair production from $\Upsilon(4S)$ and lepton universality. When combining the $K^*e^+e^-$ and $K^*\mu^+\mu^-$ modes, we assume the ratio of branching fraction of $K^*e^+e^-$ to that of $K^*\mu^+\mu^-$ to be 1.33 [7]. The combined branching fraction corresponds to muon mode. The branching fractions are found to be

$$\begin{aligned}\mathcal{B}(B \rightarrow K\ell^+\ell^-) &= (4.8_{-0.9}^{+1.0} \pm 0.3 \pm 0.1) \times 10^{-7}, \\ \mathcal{B}(B \rightarrow K^*\ell^+\ell^-) &= (11.7_{-2.7}^{+3.0} \pm 0.8 \pm 0.4) \times 10^{-7},\end{aligned}$$

where the first error is statistical, second one is due to systematic in experiment and third one is due to model dependence. These values are consistent with the SM predictions [7, 15, 16, 18] and previous results [19, 20]. The branching fractions of other decay modes are listed in Table II.

For the modes with a significance of less than 3.0, we also set 90% confidence level (C.L.) upper limits for the branching fractions. The 90% C.L. upper limit yield N is defined as $\int_0^N \mathcal{L}(n)dn = 0.9 \int_0^\infty \mathcal{L}(n)dn$. The function $\mathcal{L}(n)$ is the likelihood with signal yield n , where signal shape parameters and background shape parameters are modified by 1σ of its systematic error in the direction to increase the signal yield. The upper limits for the branching fraction are then calculated by reducing the efficiency by 1σ of its systematic error.

In summary, we have observed the electroweak penguin decay $B \rightarrow K^*\ell^+\ell^-$, for the first time. The $B \rightarrow K\ell^+\ell^-$ decay is also measured with 20% accuracy, which is better than the theoretical uncertainty. The measured branching fractions for $B \rightarrow K\ell^+\ell^-$ and $B \rightarrow K^*\ell^+\ell^-$ are in good agreement with the SM prediction [7, 15, 16, 18].

We wish to thank the KEKB accelerator group for the excellent operation of the KEKB accelerator. We acknowledge support from the Ministry of Education, Culture, Sports, Science, and Technology of Japan and the Japan Society for the Promotion of Science; the Australian Research Council and the Australian Department of Education, Science and Training; the National Science Foundation of China under contract No. 10175071; the Department of Science and Technology of India; the BK21 program of the Ministry of Education

TABLE II: Summary of the fit results and branching fractions. Number of signal yield estimated from the M_{bc} fit, detection efficiency of each mode, branching fraction obtained, 90% confidence level upper limit of the branching fraction and the significance of the signal. The first error in the signal yield and branching fraction is statistical and the second one is systematic. The third error in the branching fraction is due to model dependence. The first error in the efficiency is MC statistics and systematic error and the second one is due to model dependence.

Mode	Signal yield	Efficiency [%]	$\mathcal{B} [\times 10^{-7}]$	U.L. [$\times 10^{-7}$]	Signif.
$K^0 e^+ e^-$	$0.0^{+1.5+0.2}_{-0.9-0.4}$	$5.0 \pm 0.3 \pm 0.1$	-	5.0	-
$K^+ e^+ e^-$	$15.9^{+4.9+0.5}_{-4.2-0.6}$	$16.6 \pm 0.7 \pm 0.4$	$6.3^{+1.9}_{-1.7} \pm 0.3 \pm 0.3$	-	5.1
$K e^+ e^-$	$15.9^{+5.1+0.6}_{-4.4-0.7}$	$10.8 \pm 0.5 \pm 0.2$	$4.8^{+1.5}_{-1.3} \pm 0.3 \pm 0.1$	-	4.6
$K^{*0} e^+ e^-$	$10.2^{+4.5+0.9}_{-3.8-0.6}$	$5.2 \pm 0.3 \pm 0.1$	$12.9^{+5.7+1.2}_{-4.9-0.9} \pm 0.4$	22	2.8
$K^{*+} e^+ e^-$	$5.3^{+2.3+0.3}_{-1.6-0.4}$	$1.7 \pm 0.1 \pm 0.1$	$20.2^{+12.7+2.2}_{-10.1-2.3} \pm 0.7$	41	2.0
$K^* e^+ e^-$	$15.6^{+5.5+0.8}_{-4.8-1.0}$	$3.5 \pm 0.2 \pm 0.1$	$14.9^{+5.2+1.1}_{-4.6-1.3} \pm 0.3$	-	3.6
$K^0 \mu^+ \mu^-$	$5.7^{+3.0+0.2}_{-2.3-0.3}$	$6.7 \pm 0.4 \pm 0.3$	$5.6^{+2.9}_{-2.3} \pm 0.4 \pm 0.3$	-	3.1
$K^+ \mu^+ \mu^-$	$16.3^{+5.1+0.7}_{-4.5-0.9}$	$23.6 \pm 1.1 \pm 0.6$	$4.5^{+1.4}_{-1.2} \pm 0.3 \pm 0.1$	-	4.6
$K \mu^+ \mu^-$	$22.0^{+5.8+0.7}_{-5.1-0.9}$	$15.2 \pm 0.7 \pm 0.5$	$4.8^{+1.2}_{-1.1} \pm 0.3 \pm 0.2$	-	5.6
$K^{*0} \mu^+ \mu^-$	$17.1^{+5.4+0.6}_{-4.7-0.8}$	$8.5 \pm 0.5 \pm 0.4$	$13.3^{+4.2}_{-3.7} \pm 0.9 \pm 0.6$	-	4.4
$K^{*+} \mu^+ \mu^-$	$2.8^{+2.9+0.5}_{-2.3-0.6}$	$2.8 \pm 0.2 \pm 0.2$	-	18	-
$K^* \mu^+ \mu^-$	$20.0^{+5.8}_{-5.1} \pm 0.9$	$5.6 \pm 0.3 \pm 0.3$	$11.7^{+3.6}_{-3.1} \pm 0.8 \pm 0.6$	-	4.4
$K^0 \ell^+ \ell^-$	$5.7^{+3.4+0.4}_{-2.7-0.5}$	$5.9 \pm 0.4 \pm 0.2$	$3.2^{+1.9}_{-1.5} \pm 0.3 \pm 0.1$	6.2	2.3
$K^+ \ell^+ \ell^-$	$32.3^{+6.9+0.8}_{-6.2-1.0}$	$20.1 \pm 0.9 \pm 0.1$	$5.3^{+1.1}_{-1.0} \pm 0.3 \pm 0.0$	-	7.0
$K \ell^+ \ell^-$	$37.9^{+7.6+0.9}_{-6.9-1.1}$	$13.0 \pm 0.6 \pm 0.2$	$4.8^{+1.0}_{-0.9} \pm 0.3 \pm 0.1$	-	7.4
$K^{*0} \ell^+ \ell^-$	$27.4^{+6.9+1.1}_{-6.2-1.0}$	-	$11.7^{+3.0}_{-2.7} \pm 0.8 \pm 0.4$	-	5.3
$K^{*+} \ell^+ \ell^-$	$8.1^{+4.3}_{-3.3} \pm 0.7$	-	$10.5^{+5.6}_{-4.3} \pm 1.1 \pm 0.3$	19	2.2
$K^* \ell^+ \ell^-$	$35.8^{+7.6+1.3}_{-6.9-1.2}$	-	$11.5^{+2.6}_{-2.4} \pm 0.7 \pm 0.4$	-	5.9

of Korea and the CHEP SRC program of the Korea Science and Engineering Foundation; the Polish State Committee for Scientific Research under contract No. 2P03B 01324; the Ministry of Science and Technology of the Russian Federation; the Ministry of Education, Science and Sport of the Republic of Slovenia; the National Science Council and the Ministry of Education of Taiwan; and the U.S. Department of Energy.

* on leave from Fermi National Accelerator Laboratory, Batavia, Illinois 60510

† on leave from University of Pittsburgh, Pittsburgh PA 15260

‡ on leave from Nova Gorica Polytechnic, Nova Gorica

[1] K. Abe *et al.* (The Belle Collaboration), *Phys. Lett. B* **511**, 151 (2001).

[2] S. Chen *et al.* (CLEO Collaboration), *Phys. Rev. Lett.* **87**, 251807 (2001).

[3] R. Barate *et al.* (ALEPH Collaboration), *Phys. Lett. B* **429**, 169 (1998).

[4] T. Besmer, C. Greub, T. Hurth. CERN-TH-2001-136, BUTP-01-12, ZU-TH-15-01,

- hep-ph/0105292; M. Ciuchini *et al.*, *Nucl. Phys. B* **534**, 3 (1998); C. Bobeth, M. Misiak and J. Urban, *Nucl. Phys. B* **567**, 153 (2000); F. Borzumati *et al.*, *Phys. Rev. D* **62**, 075005 (2000); T. Goto *et al.*, *Phys. Rev. D* **58**, 094006 (1998).
- [5] K. Abe *et al.* (The Belle Collaboration), *Phys. Rev. Lett.* **88**, 021801 (2002).
- [6] J. Kaneko *et al.* (The Belle Collaboration), *Phys. Rev. Lett.* **90**, 021801 (2003).
- [7] A. Ali *et al.*, *Phys. Rev. D* **66**, 034002 (2002).
- [8] E. Lunghi, arXiv:hep-ph/0210379.
- [9] E. Lunghi *et al.*, *Nucl. Phys. B* **568**, 120 (2000); J. L. Hewett and J. D. Wells, *Phys. Rev. D* **55**, 5549 (1997); A. Ali, G. F. Giudice and T. Mannel, *Z. Phys. C* **67**, 417 (1995); N. G. Deshpande, K. Panose and J. Trampetić, *Phys. Lett. B* **308**, 322 (1993); A. Ali, T. Mannel and T. Morozumi, *Phys. Lett. B* **273**, 505 (1991); B. Grinstein, M. J. Savage and M. B. Wise, *Nucl. Phys. B* **319**, 271 (1991); W. S. Hou, R. S. Willey and A. Soni, *Phys. Rev. Lett.* **58**, 1608 (1987).
- [10] KEKB B Factory Design Report, KEK Report 95-7 (1995), unpublished; Y. Funakoshi *et al.*, Proc. 2000 European Particle Accelerator Conference, Vienna (2000).
- [11] A. Abashian *et al.* (The Belle Collaboration), *Nucl. Instrum. Methods A* **479**, 117 (2002).
- [12] Charge conjugate modes are implied throughout this paper.
- [13] R. A. Fisher, *Ann. Eugen.* **7**, 179 (1936); M. C. Kendall and A. Stuart, *The Advanced Theory of Statistics*, Second Edition (Hafner, New York, 1968) Vol III.
- [14] G. Fox and S. Wolfram, *Phys. Rev. Lett.* **41**, 1581 (1978).
- [15] D. Melikhov, N. Nikitin and S. Simula, *Phys. Lett. B* **410**, 290 (1997).
- [16] P. Colangelo *et al.*, *Phys. Rev. D* **53**, 3672 (1998), Erratum-ibid.D57:3186,1998.
- [17] H. Albrecht *et al.* (ARGUS Collaboration), *Phys. Lett. B* **241**, 278 (1990).
- [18] M. Zhong, *et al. Int. J. Mod. Phys. A* **18**, 1959, (2003); T. M. Aliev, C. S. Kim, Y. G. Kim, *Phys. Rev. D* **62**, 014026 (2000); P. Colangelo *et al. Eur. Phys. J C* **8**, 81,(1999); G. Burdman, *Phys. Rev. D* **52**, 6400 (1995); C. Greub, A. Ioannissian and D. Wyler, *Phys. Lett. B* **346**, 149 (1995); W. Jaus and D. Wyler, *Phys. Rev. D* **41**, 3405 (1990); N. G. Deshpande, J. Trampetić, K. Panose, *Phys. Rev. D* **39**, 1461 (1989); N. G. Deshpande and J. Trampetić, *Phys. Rev. Lett.* **60**, 2583 (1988).
- [19] K. Abe *et al.* (The Belle Collaboration), BELLE-CONF-0241.
- [20] J. Walsh (Babar Collaboration), BABAR-CONF-02/023.